CHEMISTRY
A European Journal

A Journal of
ChemPubSoc Europe

Accepted Article

Title: Dinuclear complexes formed by hydrogen bonds: synthesis, structure and magnetic and electrochemical properties.

Authors: Alan Francis Williams, Matteo Granelli, Alan M Downward, Robin Huber, Laure Guenée, Céline Besnard, Karl W Krämer, Silvio Decurtins, Shi-Xia Liu, and Laurence K Thompson

To be cited as: *Chem. Eur. J.* 10.1002/chem.201700591

Link to VoR: http://dx.doi.org/10.1002/chem.201700591

Supported by
ACES

WILEY-VCH

10.1002/chem.201700591

WILEY-VCH

Dinuclear complexes formed by hydrogen bonds: synthesis, structure and magnetic and electrochemical properties.

Matteo Granelli[§[a]], Alan M. Downward[§[a]], Robin Huber[[a]], Laure Guénée[[b]], Céline Besnard[[b]]
Karl W. Krämer[[c]], Silvio Decurtins[[c]], Shi-Xia Liu[[c]], Laurence K. Thompson[[d]] and Alan F. Williams[[a],*]

In memoriam Howard Flack

§ These two authors contributed equally to this work.
[a] Department of Inorganic and Analytical Chemistry, University of Geneva, 30 quai Ernest Ansermet, CH-1211 Geneva 4, Switzerland
[b] Laboratory for X-ray Crystallography, University of Geneva, 24 quai Ernest Ansermet, CH-1211 Geneva 4, Switzerland
[c] Departement für Chemie und Biochemie, Universität Bern, Freiestrasse 3, CH-3012, Switzerland
[d] Department of Chemistry, Memorial University of Newfoundland, St. John's, NL A1B 3X7 Canada

Abstract: The synthesis is reported of a series of homo- and hetero-dinuclear octahedral complexes of the ligand **1**, 1,2-bis(1-methyl-benzimidazol-2-yl) ethanol, where the two metal centres are linked by hydrogen bonds between coordinated alcohols and coordinated alkoxides. Homonuclear divalent M(II)M(II), mixed valent M(II)M(III) and heteronuclear M(II)M'(III) species are prepared. The complexes have been characterised by X-ray crystallography and show unusually short O…O distances for the hydrogen bonds. Magnetic measurements show the hydrogen bond bridges can lead to ferromagnetic or antiferromagnetic coupling. The electrochemistry of the dinuclear species is significantly different from the mononuclear systems: the latter show irreversible waves in cyclic voltammograms as a result of the need to couple proton and electron transfer. The dinuclear species, in contrast, show reversible waves which are attributed to rapid intramolecular proton transfer facilitated by the hydrogen bonded structure.

Introduction

The study of dinuclear transition metal complexes has attracted considerable attention in recent years by virtue of the various types of interaction possible between metal centres. Biology uses such systems extensively, notably in enzymes such as cytochrome c oxidase[1] or methane monoxygenase.[2] The simplest synthetic route to these complexes involves using ligands which can bind simultaneously to two metals such as pyrazine, or even simple halogen or hydroxo ligands. Greater control over the synthesis may be achieved by more sophisticated ligand design. A typical ligand will contain distinct metal binding sites connected by a linking group which, in the most favourable cases, allows control of metal-metal distances and of the electronic properties of the coordinated ions. Examples of such ligands are widespread in current literature.[3] An alternative strategy for the synthesis of dinuclear complexes, which we believe to have been less investigated, is the association of preformed mononuclear complexes into dinuclear (or, in principle, polynuclear) complexes, and it is this approach which is the subject of the present manuscript.

We will consider the formation of dinuclear complexes by hydrogen bonding between two mononuclear complexes. We present synthetic routes for homo- and heterodinuclear complexes. The structures obtained here are compared to those available in the literature and suggest that such complexes can show hydrogen bonding interactions that are sufficiently strong not to dissociate in solution. We report on the magnetic coupling between the two centres and the electrochemistry of the complexes in solution. It is found that the hydrogen bonded dimers show very different electrochemical behaviour from the mononuclear complexes and offer a simple and efficient means of coupling proton transfer to electron transfer.

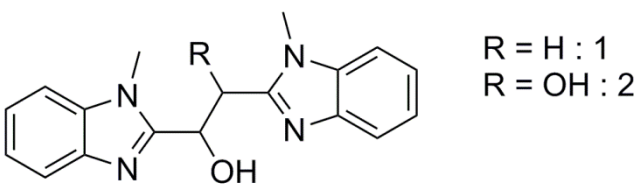

Scheme 1. Ligands referred to in this work.

The systems we have studied use the ligand **1** (Scheme 1) which is readily synthesised in enantiomerically pure form from malic acid. It carries three functions able to bind metal ions: two benzimidazoles and one alcohol. We have previously studied this ligand in connection with the formation of tetranuclear cubanes where the alcohol function is completely deprotonated and acts as a triply bridging ligand.[4] The non-methylated form of **1** has been studied by Reedijk[5] and we have studied mononuclear[6] and cubane[7] complexes of the related ligand **2** (Scheme 1) derived from tartaric acid. We were interested to examine simple complexes of the type $[M(\mathbf{1})_2]^{n+}$ where the ligands acts as a tridentate facially coordinating ligand, and in the course of this work discovered the dimers which are the subject of this work. The chemistry of the mononuclear complexes will be reported elsewhere.[8]

Results

Homonuclear dimer synthesis.

When an acidified solution of a divalent metal (Mn, Co, Ni) with two equivalents of ligand **1** is titrated with base, potentiometry shows the successive formation of $[M(\mathbf{1})]^{2+}$ and $[M(\mathbf{1})_2]^{2+}$. If excess base is added to the solution containing $[M(\mathbf{1})_2]^{2+}$ a further deprotonation is observed around pH 6.5 (Figure S1) corresponding to one equivalent of protons per metal. This is attributed to deprotonation of a coordinated alcohol function of the ligand whose pK_a is lowered significantly by complexation to the metal. We will denote the deprotonated ligand as **1**-H. No further deprotonation is observed below pH 11 indicating that only one alcohol proton may be removed. Similar behaviour was observed previously with ligand **2** and the dinuclear complex $[Ni_2(\mathbf{2}\text{-H})_2(\mathbf{2})_2]^{2+}$ could be crystallised, and was characterised by X-ray crystallography[6].

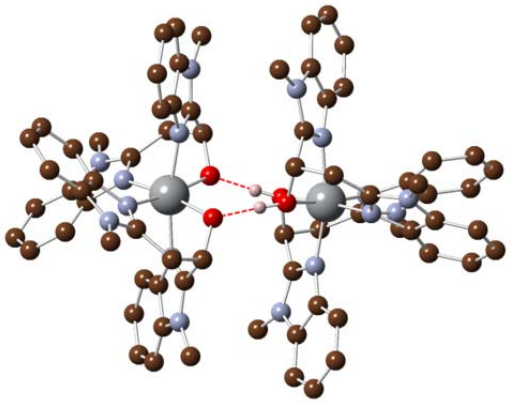

Figure 1. Structure of the $[Ni_2(S\text{-}\mathbf{1}\text{-H})_2(S\text{-}\mathbf{1})_2]^{2+}$ dimer in the compound $[Ni(II)(S\text{-}\mathbf{1}\text{-H})(S\text{-}\mathbf{1})]_2(ClO_4)_2\ 2CH_2Cl_2$. Hydrogens other than those involved in the hydrogen bond have been omitted. See text for qualification concerning the hydrogen positions.

With ligand **1** we were able to crystallise the perchlorate salt of the enantiopure complex $[Ni_2(S\text{-}\mathbf{1}\text{-H})_2(S\text{-}\mathbf{1})_2]^{2+}$ and determine its structure by X-ray crystallography (Figure 1). Details of the X-ray crystal structure determinations are given in table S1, and selected bond distances and angles in table S2. Each nickel

ion shows octahedral coordination with the ligands bound in a tridentate, facially coordinating, manner. The two alcohol functions are in *cis*- positions. The two crystallographically distinct nickel ions lie on a crystallographic twofold axis so that the two ligands on each metal are equivalent. There are no significant differences between the geometries of the two [Ni(*S*-**1**-H)(*S*-**1**)]$^+$ units. These two units are held together by hydrogen bonds between the alcohol function on one complex and the deprotonated alcohol function of the other, as shown in Scheme 2.

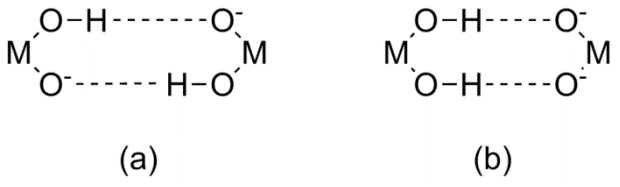

Scheme 2. Hydrogen bonding motifs in dinuclear complexes.

Two motifs are possible as shown in (a) and (b); we believe that (a) is the more plausible for the homonuclear species such as the dinickel species, but the crystallographic symmetry imposes the motif (b). Probably the hydrogen ion is disordered between the two sites. The formation of the hydrogen bonded dimer explains the absence of a second deprotonation in the potentiometry experiment since the remaining alcohol proton is retained by the hydrogen bonding. The dinuclear cobalt(II) complex [Co_2(*S*-**1**-H)$_2$(*S*-**1**)$_2$]$^{2+}$ may be prepared as for nickel(II) and was characterised by X-ray crystallography.

Heteronuclear dimers

If the same route used for nickel and cobalt is followed for manganese(II), red crystals of the mixed valence complex [Mn(II)(*S*-**1**)$_2$Mn(III)(*S*-**1**-H)$_2$](ClO$_4$)$_3$·3H$_2$O·CH$_2$Cl$_2$ were obtained. X-ray crystallography confirmed the structure as similar to the nickel dimer discussed above, but with the hydrogen bonding motif (b) in Scheme 2. The ligands bound to Mn(III) are fully deprotonated. The Mn(II) and Mn(III) sites may be distinguished clearly by the metal-ligand bond distances and the Jahn-Teller distortion expected for the Mn(III) site (Table 1).

Bond	Mn(II)	Mn(III)
Mn-N_{ax}	2.226(5)	2.277(4)
	2.237(5)	2.288(4)
Mn-N_{eq}	2.209(5)	2.030(4)
	2.215(5)	2.038(5)
Mn-O	2.184(5)	1.905(4)
	2.250(5)	1.916(4)
Mean M-L	2.220	2.076

Table 1. Bond distances (Å) for the two metal sites in [Mn(II)(*S*-**1**)$_2$Mn(III)(*S*-**1**-H)$_2$](ClO$_4$)$_3$·3H$_2$O·CH$_2$Cl$_2$. N_{ax} refers to nitrogens out of the MnN_2O_2 plane, N_{eq} to those lying in the plane.

Titration of an acid solution of iron(III) and two equivalents of ligand **1** showed that both alcohol protons are lost from the complex at low pH (Figure S1), in agreement with the observation by ESI-MS of the doubly deprotonated cation [Fe(*S*-**1**-H)$_2$]$^+$. This is in full agreement with the much greater tendency to hydrolysis of an M(III) cation compared to a M(II) cation[9] and supports the formulation [Mn(II)(*S*-**1**)$_2$Mn(III)(*S*-**1**-H)$_2$]$^{3+}$ observed by crystallography. In this case the hydrogen bond donor [Mn(II)(*S*-**1**)$_2$]$^{2+}$ has a much higher pK_a than the acceptor [Mn(III)(*S*-**1**-H)$_2$]$^+$ and the O—O distances are longer.

The formation of the mixed valence Mn(II)Mn(III) species led us to investigate the possible selective formation of heteronuclear species. Indeed mixture of a solution of [Fe(*S*-**1**-H)$_2$]$^+$ (formed by simple mixing of iron(III) perchlorate and ligand S-**1**) and a solution of [Ni(*S*-**1**)$_2$]$^{2+}$ gave rapid precipitation of the heteronuclear species [Ni(II)(*S*-**1**)$_2$Fe(III)(*S*-**1**-H)$_2$](ClO$_4$)$_3$·2MeCN and a similar reaction using [Mn(*S*-**1**)$_2$]$^{2+}$ gave [Mn(II)(*S*-**1**)$_2$Fe(III)(*S*-**1**-H)$_2$](ClO$_4$)$_3$·2MeCN. Both compounds were characterised by X-ray crystallography, and were found to be isomorphous with the mixed valence Mn(II)Mn(III) species. A similar route was used to prepare [Co(II)(*S*-**1**)$_2$Fe(III)(*S*-**1**-H)$_2$](ClO$_4$)$_3$.CH$_2$Cl$_2$. Finally we could prepare a mixed valence cobalt complex [Co(II)(*S*-**1**)$_2$Co(III)(*S*-**1**-H)$_2$](ClO$_4$)$_3$·2CH$_2$Cl$_2$ by oxidising a basic solution of [Co(*S*-**1**)$_2$]$^{2+}$ with hydrogen peroxide. Six of the eight dimers we prepared were characterised by X-ray crystallography. All complexes were studied by IR spectroscopy in the solid state, UV-visible and CD spectroscopy in solution and ESI mass spectrometry in solution. The IR spectra were all very similar supporting the dimer structure for the compounds not characterised by X-ray crystallography. The UV-visible and CD spectra were those expected for the constituent [M(*S*-**1**)$_2$]$^{2+}$ and [M(*S*-**1**-H)$_2$]$^+$ complexes,[8] and showed no signs of strong electronic interactions between the two components. In the mixed valence complexes [Mn(II)(*S*-**1**)$_2$Mn(III)(*S*-**1**-H)$_2$]$^{3+}$ and [Co(II)(*S*-**1**)$_2$Co(III)(*S*-**1**-H)$_2$]$^{3+}$ no intervalence transfer band was seen. The ESI mass spectra showed the presence of [M'(*S*-**1**-H)$_2$]$^+$ ions in the M(II)M'(III) complexes. The ion [M(*S*-**1**-H)$_2$ + H]$^+$ was observed for the M(II) ions, together with the rearrangement cubane product [M_4((*S*-**1**-H)$_4$(AcO)$_2$]$^{2+}$ probably arising from the undesired presence of acetic acid in the instrument.

Structural analysis

The six crystal structures obtained in this work show features of interest which merit comparative discussion. All show the same basic structure observed for the dinickel complex shown in Figure 1, with the double hydrogen bond bridge illustrated in Scheme 2. The observed pK_a values of the alcohol ligand lead us to assign motif (a) to the M(II)M(II) species and motif (b) to the M(II)M'(III) complexes.

The O…O distances of the hydrogen bond bridges are unusual in being very short: the three M(II)M(II) species show distances below 2.4 Å, and the M(II)M'(III) complexes are slightly longer, but all are less than 2.5 Å. Although this type of hydrogen bond interaction has often been observed in the solid state, there has been, to our knowledge, no systematic study of its occurrence. We therefore carried out a search in the Cambridge Structural Database (CSD) for the motif M-O-H…O-M and details are given in the supplementary material. Complexes containing coordinated water were excluded to limit the systems to those comparable with ligands **1** and **2**. Even with these restrictions, 158 examples were found for homonuclear interactions. A histogram of the observed O…O distances is given in Fig. 2 and shows that the distribution is bimodal.

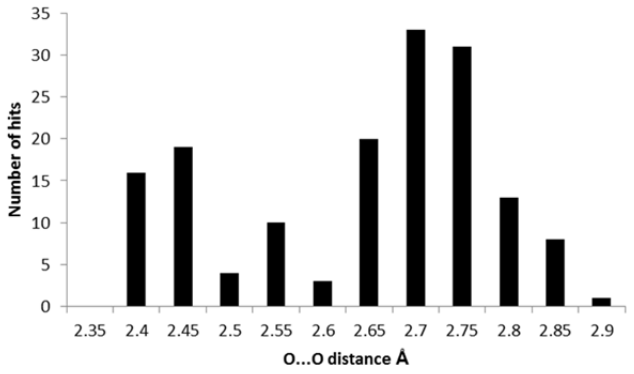

Figure 2. Histogram of the distribution of O…O distances observed in the search for the motif M-O-H…O-M. The data are grouped in bins of 0.05 Å, the bin marked 2.45 containing values between 2.425 and 2.475 Å

Most of the occurrences of this motif (roughly 80%) show a normal distribution around a distance of 2.75 Å, a perfectly reasonable value for an H-bond distance. There is however a significant separate population showing much shorter distances, in the range 2.4 – 2.5 Å, as seen for $[Ni_2(S\text{-}\mathbf{1}\text{-}H)_2(S\text{-}\mathbf{1})_2]^{2+}$. Examination of these 35 examples shows that they all contain pairs where the hydrogen bond acceptor is the conjugate base of the hydrogen bond donor, a situation which is known to favour strong hydrogen bonds.[10]. We will refer to these examples as very short hydrogen bonds since they are approximately 0.3 Å shorter than the more normal ones. There may be one, two or three very short bonds between two metal centres, and there are also cases where chains or cycles are formed using these very short bonds, but there appears to be no significant effect of the number of interactions on the O…O distances. The dimer involving two very short bonds, as observed for $[Ni_2(S\text{-}\mathbf{1}\text{-}H)_2(S\text{-}\mathbf{1})_2]^{2+}$, appears to be the most common interaction. Unfortunately there is usually no mention as to whether the interaction persists in solution, although in one case this has definitely been shown to be the case.[11]

For the M(II)M(II) complexes studied here the three structures all show very short distances, less than 2.4 Å, and are among the shortest recorded. The hydrogen bond acceptor is the conjugate base of the hydrogen bond donor. For the M(II)M(III) complexes the acid-conjugate base condition is no longer met, but the H bond donor may reasonably assumed to be more acid than for the mono deprotonated complex in motif (a) while the acceptor will be less basic because of the higher charge of the metal. The consequence of this is that the difference in pK_a of donor and acceptor may not be very great. In any event, the O…O distances, all less than 2.5 Å, although slightly greater than for the M(II)M(II) complexes, are still much shorter than the normal distance around 2.75 Å. The electrochemistry discussed below indicates strongly that the dimers persist in solution in polar solvents.

The coordination of the metal ions is essentially the same in all complexes. The ligands bind with the six-membered chelate ring in the N_2O_2 plane and the five-membered chelate rings perpendicular to this plane. All complexes have a crystallographic or non-crystallographic two-fold symmetry axis bisecting the O-M-O angle. The slight variations in structure are those to be expected for different ionic radius and oxidation state.

The crystal packing of all six structures is very similar. The structure of the complexes results in the polar alcohol/alkoxide groups lying at the centre of the dinuclear complex so that the exterior is essentially non-polar. The cationic complexes then pack in layers with the metal-metal axes parallel in the plane (Figure S2). The metrics of these layers are essentially the same for all structures. The anions and solvent molecules lie in between the layers. To investigate stereoselectivity, we reacted nickel(II) with a racemic mixture of *S*-**1** and *R*-**1**. We found the crystalline product to contain equal amounts of $[Ni_2(S\text{-}\mathbf{1}\text{-}H)_2(S\text{-}\mathbf{1})_2]^{2+}$ and $[Ni_2(R\text{-}\mathbf{1}\text{-}H)_2(R\text{-}\mathbf{1})_2]^{2+}$; we could find no evidence for complexes or dimers containing mixtures of enantiomers. In this structure alternate layers of complexes contain all S or all *R* complexes and there is thus enantioselectivity in the packing of the complexes in the layers.

Magnetic coupling in hydrogen bridged dimers.

These complexes afford a simple synthetic route to homonuclear and heteronuclear hydrogen bridged dimers, and it seemed interesting to investigate the possibilities of magnetic coupling through these bridges. Magnetic coupling through hydrogen between two paramagnetic ions has been reported previously in the literature for several types of complex. The first studied were dinuclear chromium(III) complexes linked by single, double or triple Cr-OH…H_2O-Cr bridges[12]. Antiferromagnetic interactions of varying strength are observed. These systems are close to those studied here in that the hydrogen bond is between a hydroxide ion bound to one metal and a water molecule (the conjugate acid) bound to another metal. The O…O distances are consequently short, typically in the range 2.4 – 2.5 Å that we classified as very strong hydrogen bonds. There are many examples from copper(II) chemistry.{Plass, 2001 #39;Okazawa, 2009 #20;O'Neal, 2014 #27;De Munno, 1994 #4846} Coupling through Mn-Cl…HC bridges has been reported for manganese single molecule magnets.[14] Coupling through hydrogen bond bridges has also been reported for a number of manganese(II), iron(III), cobalt(II) and nickel(II) complexes.[15] Theoretical treatments have been made for copper(II)[16] and Alvarez and co-workers extended their treatment to mixed metal systems.[17] For the moment, no clear overall picture is available; antiferromagnetic and ferromagnetic coupling has been observed, and coupling constants vary widely

We have studied the magnetic susceptibility of three of the heteronuclear dimers: $[Mn(S\text{-}\mathbf{1})_2][Fe(S\text{-}\mathbf{1}\text{-}H)_2](ClO_4)_3{\cdot}CH_3CN{\cdot}2H_2O$, $[Mn_2(S\text{-}\mathbf{1}\text{-}H)_2(S\text{-}\mathbf{1})_2](ClO_4)_3{\cdot}2CH_2Cl_2$ and $[Fe(S\text{-}\mathbf{1}\text{-}H)_2][Co(S\text{-}\mathbf{1})_2](ClO_4)_3{\cdot}2CH_2Cl_2{\cdot}EtOH$. We have previously reported on the magnetic susceptibility of a dinickel(II) complex of the non-methylated ligand similar to ligand **2** which has a similar structure to the dinickel(II) complex of ligand **1**. [6]

In the following discussion we will refer to the four complexes only by the metal ions, i.e. MnMn or MnFe.

The magnetic susceptibility data for a polycrystalline sample of the MnMn compound are displayed as plots of χ_m *vs T* and $\chi_m T$ *vs T* in Figure 3. Upon cooling, the $\chi_m T$ *vs T* plot shows a constant value of 7.7 cm^3 K mol^{-1} ($\chi_m T$ calc. = 7.4 cm^3 K mol^{-1} for $S_1 = 5/2$, $S_2 = 2$, $g = 2$) down to about 70 K, followed by a sharp increase to 18.5 cm^3 K mol^{-1} at 1.9 K. These data clearly indicate ferromagnetic coupling between the two spin centers. An isotropic spin exchange approach has been used to evaluate the ($S_1 = 5/2$, $S_2 = 2$) coupling:

$$H_{ex} = -J\{S_1 \cdot S_2\} \quad (1)$$

The magnetic data were fitted to the exchange Hamiltonian (eq. 1) using MAGMUN4.1[18], which generates the appropriate spin states and their energies prior to regression to the model. A reasonable fit was obtained with g = 2.01(3), J = 1.58(8) cm^{-1}, ρ = 0.002 (paramagnetic impurity fraction), 10^2R = 14.3 (R = $[\Sigma(\chi_{obs} - \chi_{calc})^2/\Sigma\chi_{obs}^2]^{1/2}$).

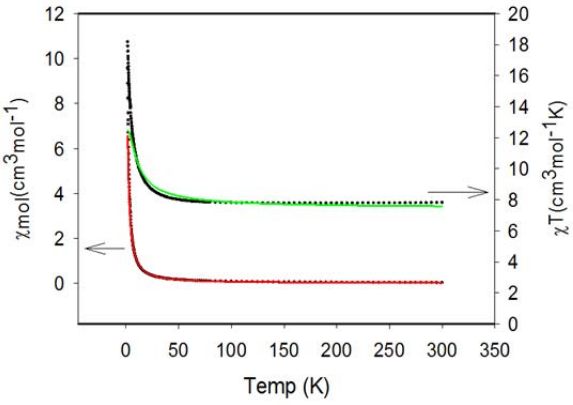

Figure 3. Thermal variation of χ_m and $\chi_m T$ for $[Mn_2(S\text{-}\mathbf{1}\text{-H})_2(S\text{-}\mathbf{1})_2](ClO_4)_3{\cdot}2CH_2Cl_2$; the red (χ_m) and green ($\chi_m T$) lines are fits according to eq 1. [18]

The magnetization data for MnMn at 1.9 K show that at high field the system approaches saturation with a value of about 8.8 Nβ (Figure 4), indicative of a high spin ground state. Fitting to the appropriate magnetization model gave g = 2.0, T = 1.9 K, S = 9/2 (10^2R = 7.3), in agreement with ferromagnetic exchange.

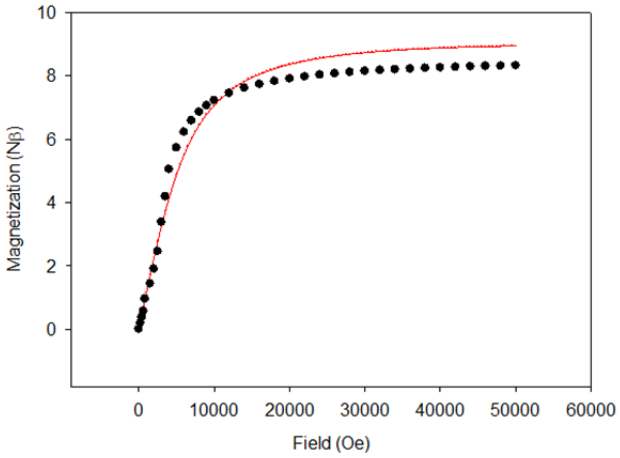

Figure 4. Magnetization *vs* field at 1.9 K for $[Mn_2(S\text{-}\mathbf{1}\text{-H})_2(S\text{-}\mathbf{1})_2](ClO_4)_3{\cdot}2CH_2Cl_2$. The red line is a fit to the magnetization model.[18]

The magnetic susceptibility data for a polycrystalline sample of MnFe are displayed as plots of χ_m *vs* T and $\chi_m T$ *vs* T in Figure 5. Upon cooling, the $\chi_m T$ *vs* T plot shows decreasing values, starting at 9.1 cm^3 K mol^{-1} at 300 K ($\chi_m T$ calc. = 8.8 cm^3 K mol^{-1} for $S_1 = S_2$ = 5/2, g = 2) and reaching 1.1 cm^3 K mol^{-1} at 1.9 K. These data clearly indicate antiferromagnetic coupling between the two spin centres. The magnetic data were fitted to eq. 1 ($S_1 = S_2$ = 5/2) using MAGMUN4.1.[18] to give g = 2.003(3), J = -1.26(1) cm^{-1}, TIP = 0.000018 cm^{3}mol^{-1}, ρ = 0.0003, θ = 0.12 K, 10^2R = 2.83. The best fit was obtained using additional parameters (θ = Weiss-like temperature correction). However the low temperature data were difficult to model, and there is a slight discrepancy between the experimental and calculated lines, possibly arising from an underestimation of the paramagnetic impurities. The M/H data at 1.9 K indicate a system with a low spin ground state as expected. No fitting of the M/H data was attempted.

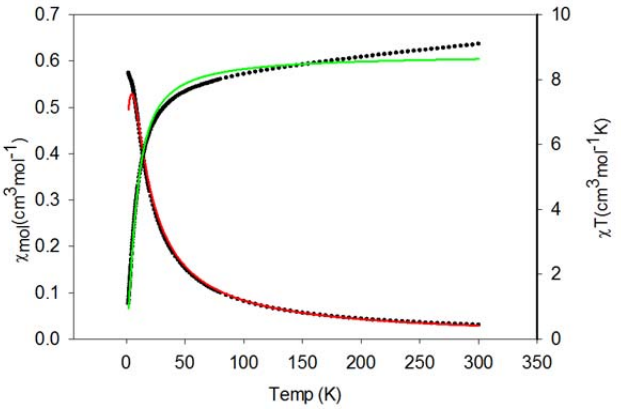

Figure 5. Thermal variation of χ_m and $\chi_m T$ for $[Fe(S\text{-}\mathbf{1}\text{-H})_2][Mn(S\text{-}\mathbf{1})_2](ClO_4)_3{\cdot}CH_3CN{\cdot}2H_2O$; the red ($\chi_m$) and green ($\chi_m T$) lines are fits according to eq 1.

The χT plot for FeCo shows a slow fall from room temperature to around 50 K after which it falls away rapidly to around 2 cm^{3}mol^{-1}K at 3 K (Figure S3). In view of the complexity introduced by the spin orbit coupling in the cobalt(II) system no fit was attempted, but the coupling would appear to be antiferromagnetic. The lowest χT value is well below that expected for a high spin Fe(III) and a Co(II) ion without interaction. In our previous work, a NiNi dimer was found to show antiferromagnetic coupling with a J value estimated as -4.7(1) cm^{-1}.[6]

There are no significant structural differences between MnMn, MnFe, FeNi, and we may reasonably assume that the structure of FeCo will not show any significant differences. The structure for NiNi[6] is equally similar, although, as we observed for the M(II)M(II) structures above, the O…O distance at 2.399(1)Å is about 0.07Å shorter than for the M(II)M(III) systems. The very different J values do not therefore seem to have structural origins. The total magnetic exchange interaction within a dimer compound expressed by the J parameter results from the combination of many electron-electron interactions with individual parameters J_{ab} (centre a and centre b) and it is in general not straightforward to elucidate the sign and magnitude of J[19].

Electrochemistry

The potentiometric and synthetic studies combined with the X-ray structural assignments allow us to identify the four species A, B, C, and D shown in Scheme 3.

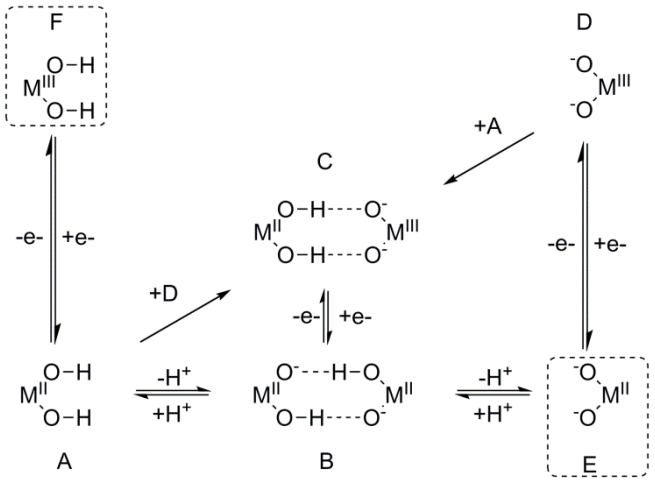

Scheme 3. Different ML_2 species in this work positioned according to their degree of oxidation (vertical axis) and protonation (horizontal axis). Species E and F have not been observed.

Species **A** has been observed as *trans*- isomers[8] and by Reedijk as a *cis*- isomer with nickel(II).[5] **B** and **C** have been characterised by X-ray crystallography and the transformation of **A** into **B** was shown by potentiometry. **D** has been characterized structurally as a *trans*- isomer with Co(III)[8] and its existence has been shown by potentiometry and the ion has been observed by ESI-MS for cobalt(III), manganese(III) and iron(III). The reaction between **A** and **D** has been shown to give **C**. For cobalt and manganese, solutions of **B** oxidise slowly in air to give mixed valence dimers **C**.

Simple one electron oxidation of the mononuclear complex **A** or one electron reduction of **D** would lead to the species **F** and **E** respectively. Neither of these species has been observed in solution, and potentiometry suggests that they are both unstable and consequently of high energy. We may therefore expect that oxidation or reduction of the mononuclear species will be coupled with proton transfer as is common for redox couples involving metal ions. Recent years have seen growing interest in Proton Coupled Electron Transfer (PCET) and it has been the subject of many reviews: general[20], specifically of metal complexes[21], oxygen activation[22], inside proteins[23], after photoexcitation[24] and from a theoretical point of view[25]. For the dimers the redox process involves species **B** and **C** and needs no external source of protons, although according to our assignment of the H-bonds, an intramolecular proton transfer is necessary. We have studied the redox transformations between these different species using cyclic voltammetry.

A comparison of cyclic voltammograms of the mononuclear complex $[Mn(II)(S\text{-}\mathbf{1})_2]^{2+}$ and the manganese mixed valence complex $\{[Mn(II)(S\text{-}\mathbf{1})_2][Mn(III)(S\text{-}\mathbf{1}\text{-}H)_2]\}^{3+}$ is shown in Figure 6. The mononuclear complex shows no sign of oxidation below + 1.0 V, and a weak peak on reduction around + 0.6 V which we suspect to arise from traces of the mixed valence compound **C** formed during the oxidation scan. The mixed valence complex $\{[Mn(II)(S\text{-}\mathbf{1})_2][Mn(III)(S\text{-}\mathbf{1}\text{-}H)_2]\}^{3+}$ is very different and shows a quasi-reversible peak at $E_{½}$ = ½(E_{pa} + E_{pc}) = +0.68 V, ΔE = (E_{pa} - E_{pc}) = 140 mV, Figure 6.

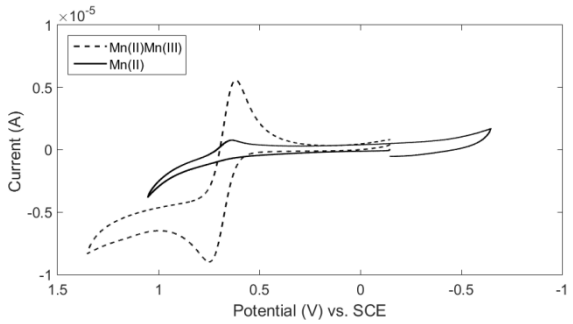

Figure 6. Cyclic voltammograms of $\{[Mn(II)(S\text{-}\mathbf{1})_2][Mn(III)(S\text{-}\mathbf{1}\text{-}H)_2]\}^{3+}$ (dashed line) and $[Mn(II)(S\text{-}\mathbf{1})_2]^{2+}$ (full line) in acetonitrile solution.

Figure 7 shows a comparison of the voltammograms of the mononuclear complex $[Fe(III)(S\text{-}\mathbf{1}\text{-}H)_2]^{+}$ and the heteronuclear species $\{[Ni^{II}(S\text{-}\mathbf{1})_2][Fe^{III}(S\text{-}\mathbf{1}\text{-}H)_2]\}^{3+}$. As expected the mononuclear complex shows irreversible behavior, being reduced only at a very negative potential (-0.93V) and showing a broad reoxidation potential around -0.54 V. The heteronuclear species $\{[Ni^{II}(S\text{-}\mathbf{1})_2][Fe^{III}(S\text{-}\mathbf{1}\text{-}H)_2]\}^{3+}$ is again quite different, showing a quasi-reversible peak at $E_{½}$ = -0.21 V, ΔE = 80 mV). The peak may be attributed to the couple Ni(II):Fe(III)/ Ni(II):Fe(II) and corresponds to species **C** and **B** in Scheme 3. No redox activity associated with the nickel(II) ion is expected and none is observed. The difference in potential of 0.91 V for the couple **C**/**B** for the iron and manganese complexes is consistent with the relative oxidizing power of Mn(III) and Fe(III). This assignment is supported by the voltammograms of the closely related complexes $\{[Mn(II)(S\text{-}\mathbf{1})_2][Fe(III)(S\text{-}\mathbf{1}\text{-}H)_2]\}^{3+}$ and $\{[Co(II)(S\text{-}\mathbf{1})_2][Fe(III)(S\text{-}\mathbf{1}\text{-}H)_2]\}^{3+}$ which show the same quasi-reversible peak (Figure S4). The Mn(II):Fe(III) complex gave $E_{½}$ = -0.23 V, ΔE = 123 mV and Co(II):Fe(III) $E_{½}$ = -0.24 V, ΔE = 78 mV, not significantly different from the Ni(II):Fe(III) species. This is what one would expect for reduction of the same Fe(III)/Fe(II) couple in a system where the interaction between the two metals is weak.

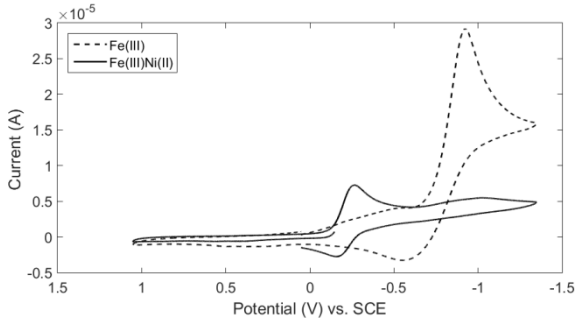

Figure 7. Cyclic voltammograms of $[Fe^{III}(S\text{-}\mathbf{1}\text{-}H)_2]^{+}$ (dashed line) and $\{[Ni^{II}(S\text{-}\mathbf{1})_2][Fe^{III}(S\text{-}\mathbf{1}\text{-}H)_2]\}^{3+}$ (full line) in acetonitrile solution.

The cobalt systems were less clear cut (Figure S5). Solutions of $[Co(III)(S\text{-}\mathbf{1}\text{-}H)_2]^{+}$ showed a reduction around -0.5 V associated with reduction of $[Co(III)(S\text{-}\mathbf{1}\text{-}H)_2]^{+}$ (type **D**). An oxidation wave

attributed to oxidation of $[Co(II)(S\text{-}\mathbf{1})_2]^{2+}$ (type **A**) was seen at +1.17 V and is also visible in the voltammogram of $\{[Co(II)(S\text{-}\mathbf{1})_2][Fe(III)(S\text{-}\mathbf{1}\text{-}H)_2]\}^{3+}$ (Figure S4) as might be expected. Solutions of the type **B** dimer $[Co(II)_2(S\text{-}\mathbf{1})(S\text{-}\mathbf{1}\text{-}H)_2]^{2+}$ showed an oxidation peak around + 0.8 V, lower than for $[Co(II)(S\text{-}\mathbf{1})_2]^{2+}$ as one might expect. If the scan was initially in the direction of reduction, no peak was observed, but if the scan began with oxidation, a reduction feature was visible around -0.5 V. It must be recalled that the Co(III)/Co(II) couple involves not only rearrangement of the coordination sphere but also a change from low spin Co(III) to high spin Co(II) and that this disfavours rapid and reversible electron transfer.

The difference between the voltammograms of the mononuclear and the dinuclear complexes establishes beyond doubt that the dimers do not dissociate under the experimental conditions. The change from irreversible kinetics in the mononuclear complexes to quasi-reversible kinetics for the dinuclear species must be associated with the ease of proton transfer. The crystal structure data for the homonuclear and heteronuclear species give a good idea of the geometric changes involved in the oxidation of **B** to **C** and the back reaction. The average O…O distances are 2.39 Å for the **B** species and 2.47 Å for the **C**. The change in O…O distance is thus of the order of 0.08 Å, about half the change in metal-ligand bond distances observed for the transition Mn(II)-Mn(III) as deduced from the bond lengths of table 2. The O-H distances obtained from X-ray crystallography are not accurate enough to measure the movement of the protons, but if we assume an O-H bond distance of 1.0 Å, then the intramolecular proton transfer needs only to take place over a distance of the order of 0.5 Å. This short distance could allow significant overlap between the O-H stretching wavefunctions of reactant and product which is favourable for concerted proton electron transfer (CPET).[25a, 26] It is therefore eminently reasonable for the kinetics for electron transfer to be much faster in the dinuclear species.

Conclusions

We have shown that ligand **1** may be used to form a variety of dinuclear complexes by deprotonation of the alcohol function to form double hydrogen-bond bridges. Both divalent M(II)M(II) and mixed valent M(II)M(III) species may easily be prepared, the latter as homo- or heteronuclear complexes. The dinuclear species do not dissociate in solution and this presumably arises from the formation of very strong hydrogen bonds as deduced from the short O…O distances in the range 2.4 – 2.5 Å. The M(II)M(III) species show slightly longer O…O distances than the M(II)M(II) but are still much shorter than normal O…O distances. The strength of the hydrogen bonds is thought to arise from the fact that the pK_a of H-bond donor and acceptor are very close and indeed equal in the homonuclear divalent complexes. A search of the Cambridge Structural Database shows many other examples of very short bonds involving acid and conjugate base pairs, but this does not appear to have been recognised as a very general effect.

The formation of the complexes is stereoselective: using a mixture of *R*- and *S*- ligands gives homochiral *RRRR*- or *SSSS*-dimers. In the solid state the homochiral complexes pack into homochiral layers. Magnetic moments show that exchange through the bridges is present, but varies considerably with the metal ions, from ferromagnetic to antiferromagnetic, even though all the evidence suggests there to be little structural difference in the bridges. Finally the hydrogen bond bridges greatly facilitate electron transfer when compared to the mononuclear species. Oxidation of the M(II)M(II) dimer to M(III)M(II) is now reversible on the time scale of cyclic voltammetry since the hydrogen bridge allows rapid intramolecular proton transfer over a short distance to give the protonation state (Scheme 3) consistent with the new oxidation states. Thus the outer sphere electron transfer to the electrode is coupled to an inner-sphere proton transfer.

Ligand **1** is versatile and can form octahedral complexes with a number of 3d metal ions; we have prepared mononuclear complexes of Cr(III), V(III) and Cd(II)[8] and no doubt dimers containing these metals could be prepared. On the basis of the structural results presented here the resulting complexes would be expected to be isostructural. This offers a route to a large number of essentially isostructural compounds with different d-electron configurations for studying magnetic exchange and the coupling of proton transfer with electron transfer. We surmise, and it is supported by the evidence of the CSD search, that any ligand where two or three alcohol functions can occupy mutually *cis*- positions may be deprotonated to form such hydrogen bridged dimers. There is in principle no reason why the ligands on the different metals need to be identical, the only requirement being that the pK_a of the alcohol or water protons should be equal or close.

Experimental Section

^{1}H-NMR and ^{13}C spectra were recorded on a Bruker Avance 400 spectrometer (400 MHz) at room temperature. Proton chemical shifts are given with respect to tetramethylsilane. High-resolution mass spectra were obtained on a QSTAR XL (AB/MSD Sciex) instrument in an ESI positive mode by the Mass Spectrometry Laboratory, University of Geneva. Low-resolution mass spectra were obtained on a Applied Biosystems Sciex API 150EX Ion Turbo Spray instrument. IR spectra were measured on a Bruker Tensor 27 equipped with a Platinum ATR module. Elemental analyses were performed using a Varian MICRO Cube instrument at the Microchemical Laboratory of the University of Geneva. The crystals used for structural determinations often contain volatile organic solvents in between the cationic layers which are lost or replaced by water on standing in air. They were removed directly from the mother liquid. Crystals used for elemental analysis were dried and consequently compositions do not invariably agree with the crystal structures. UV−vis spectra were recorded on a Perkin-Elmer Lambda 900 spectrometer with quartz cells of 1 cm of path length. CD spectra were obtained using a JASCO J-815 spectropolarimeter. Potentiometric titrations were carried out under a nitrogen atmosphere using a Metrohm 736 GP Titrino unit controlled by the programme Tinet 2.4 on a PC. Typical conditions used an initial volume of 20 ml ethanol: water 2:1 with 0.1 mmol ligand, 0.05 mmol metal salt and 0.15 mmol free acid in the solution. Ionic strength was maintained at 0.1 M with sodium perchlorate. The solution was titrated with a standard solution of NaOH 0.1 M. Cyclic voltammetry measurements used a BAS Epsilon system with platinum working and auxiliary electrodes and an Ag/AgCl reference electrode. Acetonitrile was used as solvent with Bu_4NPF_6 (0.1 M) as background electrolyte. Ferrocene was used as an internal standard, and potentials are referred to SCE. The ferrocene potential was taken to be +0.382 V.[27] The scan rate was 100 mV/s.

Magnetic susceptibility measurements were made on a Quantum Design MPMS SQUID-*XL* magnetometer under an applied magnetic field of 1000 Oe between 300 and 1.9 K. The sample was prepared in a gelatine

capsule. Diamagnetic corrections were made for the sample using the approximation -0.45 x molecular weight x 10^{-6} cm^3 mol^{-1} and the sample holder was corrected for by measuring directly the susceptibility of the empty capsule.

X-ray crystallographic intensity measurements were made with an Agilent Supernova diffractometer equipped with a CCD bidimensional detector using monochromatic Cu-Kα radiation (λ=1.54184Å). Full crystal data and structure refinement details are given in Table S1. CCDC 1528110-3, 1529058-9 contain the supplementary crystallographic data for this paper. These data can be obtained free of charge from The Cambridge Crystallographic Data Centre via www.ccdc.cam.ac.uk/data_request/cif.

Synthesis

Ligand *S*- and *R*-**1** were prepared as described previously.[4a]

$[Ni_2(S\text{-}1\text{-}H)_2(S\text{-}1)_2](ClO_4)_2\cdot 5.5H_2O$. In a test-tube, a mixture of $Ni(ClO_4)_2\cdot 6H_2O$ (39.9 mg 0.11 mmol) and *S*-**1** (66.9 mg, 0.22 mmol) was suspended in 5 ml of 50:50 EtOH/CH_2Cl_2 solution. Et_3N (220 µl, 0.5 M in EtOH, 0.11 mmol) was added, giving a clear light blue solution. In few hours, 73.9 mg of a crystalline light blue solid was formed (44%). IR (cm^{-1}) ν_{max}: 3537 (w), 3057 (w), 2945 (w), 1703 (w), 1616 (w), 1502 (m), 1479 (s), 1450 (s), 1410 (s), 1321 (s), 1288 (m), 1236 (m), 1148 (s), 1082 (w), 1007 (s), 980 (s), 918 (s), 843 (s), 804 (m), 743 (m), 621 (s), 565 (s), 527 (m), 509 (m), 482 (w), 444 (w), 326 (m), 305 (m), 274 (s), 247 (m). UV-Vis (20 °C, CH_3CN, nm) λ_{max} (ε, $M^{-1}cm^{-1}$): 256 (52600), 268 (53200), 275 (64500), 282 (64800), 355 (267), 370 (253), 390 (161), 417sh (31.2), 581 (19.5), 966 (18.4). CD (20 °C, CH_3CN, nm) λ (Δε, $M^{-1}cm^{-1}$): 259 (-62.3), 273 (-26.3), 281 (-17.6), 310 (0.11), 390 (-0.15), 572 (-0.17), 768 (-0.10). ES-MS (soft positive mode, MeCN) m/z: 669.3 (71) $[Ni(S\text{-}1\text{-}H)_2 + H]^+$, 523.3 (100) $[Ni_4(S\text{-}1\text{-}H)_4](ClO_4)(H_2O)^{3+}$, 363.1 (86) $[Ni_4(S\text{-}1\text{-}H)_4]^{2+}$. Anal. Calculated for $[Ni_2(S\text{-}1)_2(S\text{-}1\text{-}H)](ClO_4)_2\cdot 5.5H_2O$: C 52.77%, H 4.98%, N 13.68%; Found: C 52.76%, H 4.74%, N 13.45%.

$[Ni_4(R\text{-}1\text{-}H)_2(S\text{-}1\text{-}H)_2(R\text{-}1)_2(S\text{-}1)_2](ClO_4)_4\cdot 6CH_2Cl_2\cdot 2EtOH$. In a test-tube, to a mixture of $Ni(ClO_4)_2\cdot 6H_2O$ (31.9 mg 0.09 mmol), *S*-**1** (25.5 mg, 0.08 mmol) and *R*-**1** (25.5 mg, 0.08 mmol) in 5 ml of a 50:50 EtOH/CH_2Cl_2 solution was added Et_3N (250 µl, 0.5 M in EtOH, 0.09 mmol). In few hours, 45.6 mg of a crystalline light blue solid was formed (60%). IR (cm^{-1}) ν_{max}: 3510 (w), 3057 (w), 2945 (w), 1614 (w), 1502 (w), 1479 (m), 1450 (m), 1408 (m), 1321 (m), 1288 (m), 1236 (w), 1190 (w), 1148 (w), 1082 (s), 1026 (w), 1009 (w), 977 (s, br), 917 (w), 887 (w), 843 (w), 802 (w), 739 (s), 623 (m), 565 (w), 525 (w), 509 (w), 484 (w), 435 (m), 356 (w), 324 (w), 305 (w), 277 (m). Anal. Calculated for **[**$Ni_4(R\text{-}1\text{-}H)_2(S\text{-}1\text{-}H)_2(R\text{-}1)_2(S\text{-}1)_2](ClO_4)_4\cdot 6CH_2Cl_2\cdot 2EtOH$: C 50.25%, H 4.49%, N 12.18%; Found: C 50.37%, H 4.58%, N 12.22%.

$[Co_2(S\text{-}1\text{-}H)_2(S\text{-}1)_2](ClO_4)_2\cdot 2CH_2Cl_2\cdot H_2O$. In a test-tube, a mixture of $Co(ClO_4)_2\cdot 6H_2O$ (40.0 mg, 0.11 mmol) and *S*-**1** (66.5 mg, 0.22 mmol) was suspended in 5 ml of a 50:50 EtOH/CH_2Cl_2 solution. Et_3N (220 µl, 0.5 M in EtOH, 0.11 mmol) was added, yielding a clear light violet solution. In few days, 33.3 mg of a crystalline dark pink solid was formed (18%). IR (cm^{-1}) ν_{max}: 3530 (w, br), 2951 (w), 1612 (w), 1593 (w), 1483 (m), 1454 (m), 1414 (m), 1327 (m), 1288 (m), 1234 (w), 1076 (s), 1009 (s), 930 (w), 907 (w), 841 (m), 814 (m), 743 (s), 656 (w), 621 (s), 565 (m), 527 (m), 507 (w), 411 (w), 320 (w), 280 (m), 253 (m), 226 (s), 208 (s). UV-Vis (20 °C, H_2O/EtOH = 1/1, nm) λ_{max} (ε, $M^{-1}cm^{-1}$): 252 (52700), 269 (58000), 276 (68400), 282 (65800), 355 (369), 373 (370), 392 (237), 478 (97.1), 506 (92.2), 530 (85.8, sh), 1077 (20.9). CD (20 °C, CH_3CN, nm) λ (Δε, $M^{-1}cm^{-1}$): 255 (-39.1), 273 (-25.8), 280 (-19.4), 313 (-4.54), 386 (-0.71), 439 (3.16), 593 (-1.28). ESI-MS (soft positive mode, MeCN) m/z: 364.1 (56) $[Co_4(S\text{-}1\text{-}H)_4]^{4+}$, 669.3 (100) $[Co^{III}(S\text{-}1\text{-}H)_2]^+$, 787.3 (5) $[Co_4(S\text{-}1\text{-}H)_4(AcO)_2]^{2+}$, 827.3 (3) $[Co_4(S\text{-}1\text{-}H)_4](ClO_4)_2^{2+}$. Anal. Calculated for $[Co_2(S\text{-}1)_2(S\text{-}1\text{-}H)_2](ClO_4)_2\cdot 2CH_2Cl_2\cdot H_2O$: C 51.45%, H 4.66%, N 12.27%; Found: C 51.40%, H 4.72%, N 12.68%.

$[Mn_2(S\text{-}1\text{-}H)_2(S\text{-}1)_2](ClO_4)_3\cdot 2CH_2Cl_2$. Method A: 108 mg of $Mn(ClO_4)_2.6H_2O$ (0.3 mmol) and 184 mg of *S*-**1** (0.6 mmol) were dissolved in 10 ml of a 50:50 MeOH/CH_2Cl_2 solution. To this solution Et_3N (600 µl, 0.5 M in EtOH, 0.3 mmol) was added. Slow evaporation results in the formation of 157 mg of the product as a red crystalline material (157 mg, 58%). Method B: 2 mg $KMnO_4$ (0.013 mmol), 41.2 mg $Mn(ClO4)_2\cdot 6H_2O$ (0.114 mmol), and 78 mg of *S*-**1** (0.253 mmol) were placed in a 1:1 MeOH/CH_2Cl_2 solution. All reactants except for the permanganate dissolved and the solution was sealed and left to stand for at least one week, until red crystals had started to form. At this point the solution was allowed to evaporate slowly and 79 mg of product were filtered off once the volume had reduced by about half (69%). IR (cm^{-1}) ν_{max}: 3535 (w, br), 3061 (w), 2953 (w), 1614 (w), 1483 (m), 1452 (m), 1410 (m), 1317 (m), 1286 (m), 1236 (w), 1155 (w), 1068 (s), 1005 (m), 945 (w), 918 (w), 895 (w), 389 (m), 808 (m), 743 (s), 698 (w), 652 (w), 621 (s), 576 (m), 563 (m), 517 (w), 501 (w), 472 (w), 436 (m), 399 (w), 332 (w), 285 (w), 262 (w), 241 (w). UV-Vis (20 °C, MeCN, nm) λ_{max} (ε, $M^{-1}cm^{-1}$): 246 (52400), 254 (48600), 267 (53200), 274 (63600), 281 (59100), 310 (2810, sh), 411 (236), 589 (32.2), 835 (17). UV-Vis (20 °C H_2O/EtOH = 1/1, nm) λ_{max} (ε, $M^{-1}cm^{-1}$): 248 (57500), 255 (57300), 269 (60200), 276 (70300), 283 (63100), 422 (548), 555 (240). CD (20°C, CH_3CN, nm) λ (Δε, $M^{-1}cm^{-1}$): 255 (-39.1), 273 (-25.8), 280 (-19.4), 313 (-4.54), 386 (-0.71), 439 (3.16), 593 (-1.28). ESI-MS (soft positive mode, MeCN) m/z: 665.3 (95) $[Mn^{III}(S\text{-}1\text{-}H)_2]^+$, 666.5 (71) $[Mn^{II}(S\text{-}1)_2 + H]^+$, 779.5 (16) $[Mn_4(S\text{-}1\text{-}H)_4(AcO)_2]^{2+}$. Anal. Calculated for $[Mn(S\text{-}1)_2][Mn(S\text{-}1\text{-}H)_2](ClO_4)_3\cdot 2CH_2Cl_2$: C 49.34%, H 4.14%, N 12.44%; Found C 49.74%, H 3.99%, N 12.56%. UV-visible (T=25°, solid state) λ_{max}/nm (%R): 217 (77), 257 (78), 274 (75), 282 (76), 350 (90), 454 (89), 897 (91). HR-ESI-MS: 665.2175 $[Mn^{III}(S\text{-}1\text{-}H)_2]^+$ = 665.2180.

$[Mn(S\text{-}1)_2][Fe(S\text{-}1\text{-}H)_2](ClO_4)_3\cdot CH_3CN\cdot 2H_2O$. In a test-tube, to a solution of $Fe(ClO_4)_3\cdot xH_2O$ (48 mg, 0.14 mmol) and H-*S*-**1** (123 mg, 0.40 mmol) in 3 ml of 50:50 MeOH/CH_2Cl_2 was added a solution of $Mn(ClO_4)_2\cdot 6H_2O$ (36 mg, 0.10 mmol) in 2 ml of 50:50 MeOH/CH_2Cl_2. A fine crystalline orange precipitate immediately formed (110 mg). The precipitate was dissolved in MeCN and Et_2O diffused in giving 55 mg of final product as orange-brown crystals (33%). IR (cm^{-1}) ν_{max}: 3522 (w, br), 2951 (w), 1614 (w), 1483 (m), 1452 (m), 1408 (m), 1319 (m), 1288 (m), 1236 (w), 1153 (w), 1072 (s), 1007 (m), 928 (m), 893 (m), 806 (w), 743 (s), 565 (s), 550 (w), 517 (w), 498 (w), 476 (w), 442 (m), 395 (w), 326 (w), 280 (m), 247 (w), 226 (m). UV-Vis (20°C, CH_3CN, nm) λ_{max} (ε, $M^{-1}cm^{-1}$): 247 (54800), 254 (52100), 266 (53400), 274 (69300), 281 (69600), 355 (5000), 600 (31.8). CD (20 °C, CH_3CN, nm) λ (Δε, $M^{-1}cm^{-1}$): 257 (-30.3), 272 (-34.4), 279 (-28.5), 342 (-4.21), 4625 (-0.26). ES-MS (soft positive mode, MeCN) m/z: 666.5 (90) $[Fe(S\text{-}1\text{-}H)_2]^+$, 779.5 (11) $[Mn_4(S\text{-}1\text{-}H)_4(AcO)_2]^{2+}$. Anal. Calculated for $[Fe(S\text{-}1\text{-}H)_2][Mn(S\text{-}1)_2](ClO_4)_3\cdot CH_3CN\cdot 2H_2O$: C 51.99%, H 4.54%, N 13.93%; Found: C 51.91%, H 4.51%, N 13.98%.

$[Fe(S\text{-}1\text{-}H)_2][Ni(S\text{-}1)_2](ClO_4)_3\cdot 2H_2O\cdot 3.5CH_2Cl_2$. In a test-tube, a solution of $Fe(ClO_4)_3\cdot xH_2O$ (29.0 mg 0.08 mmol) and *S*-**1** (45.6 mg, 0.15 mmol) in 3 ml of a 50:50 MeOH/CH_2Cl_2 mixture was added to a solution of $Ni(ClO_4)_2\cdot 6H_2O$ (29.9 mg, 0.08 mmol) and *S*-**1** (45.6 mg, 0.15 mmol) in 3 ml of a MeOH/CH_2Cl_2 mixture. 71.8 mg of a yellow solid formed immediately (59%). Crystals suitable for X-Ray diffraction were obtained by slow diffusion of Et_2O vapours into a yellow solution of the supramolecular dimer in MeCN. IR (cm^{-1}) ν_{max}: 3543 (w, br), 3065 (w), 2949 (w), 1616 (w), 1483 (m), 1454 (m), 1412 (m), 1321 (m), 1288 (m), 1236 (w), 1074 (s, br), 1009 (m), 928 (w), 893 (w), 845 (w), 806 (w), 745 (s), 623 (s), 567 (w), 552 (w), 528 (w), 501 (w), 478 (w), 449 (m), 399 (w), 326 (w), 280 (s), 226 (m), 212 (w). UV-Vis (20 °C, CH_3CN, nm) λ_{max} (ε, $M^{-1}cm^{-1}$): 254 (52900), 281 (65400), 274 (68600), 375 (1900), 592 (22), 1030 (20). CD (20 °C, CH_3CN, nm) λ (Δε, $M^{-1}cm^{-1}$): 258 (-47.7), 272 (-38.7), 279 (-30.0), 333 (-4.0), 434 (-0.95), 568 (-0.12), 627 (0.04), 709 (-0.20). ESI-MS (soft positive mode, EtOH/CH_2Cl_2 = 1/1) m/z: 666.5 (100) $[Fe(S\text{-}1\text{-}H)_2]^+$, 669.3 (42) $[Ni(S\text{-}1)_2 + H]^+$. Anal. Calculated for $[Fe(S\text{-}1\text{-}H)_2][Ni(S\text{-}1)_2](ClO_4)_3\cdot 2H_2O\cdot 3.5CH_2Cl_2$: C 46.04%, H 4.15%, N 11.38%; Found: C 45.96%, H 4.12%, N 11.87%.

$[Fe(S\text{-}1\text{-}H)_2][Co(S\text{-}1)_2](ClO_4)_3\cdot CH_2Cl_2$. In a test-tube, to a solution of $Fe(ClO_4)_3\cdot xH_2O$ (48 mg, 0.14 mmol) and *S*-**1** (123 mg, 0.40 mmol) in 3 ml of a 50:50 $MeOH/CH_2Cl_2$ mixture was added a solution of $Co(ClO_4)_2\cdot 6H_2O$ (36 mg, 0.10 mmol) in 2 ml of a 50:50 $MeOH/CH_2Cl_2$ mixture giving a dark orange solution. Slow evaporation of the solvent led to the formation of 69 mg of orange crystals (40%). IR (cm^{-1}) ν_{max}: 3539 (w), 3061 (w), 2953 (w), 1614 (w), 1483 (m), 1454 (m), 1410 (m), 1319 (m), 1288 (m), 1236 (w), 1153 (w), 1072 (s, br), 1007 (m), 928 (w), 891 (w), 843 (w), 806 (w), 743 (s), 621 (s), 565 (w), 550 (w), 527 (w), 517 (w), 500 (w), 478 (w), 446 (m), 397 (w), 326 (w), 280 (s). UV-Vis (20 °C, CH_3CN, nm) λ_{max} (ε, $M^{-1}cm^{-1}$): 252 (53700), 274 (66500), 280 (63400), 363 (3450), 525 (180), 1078 (25.2). CD (20 °C, CH_3CN, nm) λ (Δε, $M^{-1}cm^{-1}$): 255 (-27.9), 256 (-27.6), 272 (-24.6), 278 (-19.2), 336 (-2.60), 425 (-0.93), 600 (-1.04). ES-MS (soft positive mode, MeCN) m/z: 666.7 (100) $[Fe(S\text{-}1\text{-}H)_2]^+$, 669.3 (64) $[Co^{III}(S\text{-}1\text{-}H)_2]^+$. Anal. Calculated for $[Fe(S\text{-}1\text{-}H)_2][Co(H\text{-}S\text{-}1)_2](ClO_4)_3\cdot CH_2Cl_2$: C 50.93%, H 4.22%, N 13.02%; Found: C 51.01%, H 4.49%, N 13.47%.

$[Co(S\text{-}1\text{-}H)_2][Co(S\text{-}1)_2](ClO_4)_3\cdot 1.5CH_2Cl_2\cdot 0.5EtOH$. In a test-tube, to a solution of $Co(ClO_4)_2\cdot 6H_2O$ (34.0 mg 0.09 mmol), *S*-**1** (57.2 mg, 0.19 mmol) and Et_3N (186 µl, 0.5 M in EtOH, 0.09 mmol) in 10 ml of MeCN was added a solution of H_2O_2 (26.0 µl, 3% in H_2O, 0.09 mmol). In one week the colour of the solution turned into orange-brown. The solvent was evaporated and the remaining brownish solid was dissolved in 4 ml of a $EtOH/CH_2Cl_2$ mixture. The solvent was allowed to evaporate slowly and 59.2 mg of a pink-violet crystalline solid were formed (72%). IR (cm^{-1}) ν_{max}: 3525 (w, br), 3057 (w), 2951 (w), 1614 (w), 1506 (w), 1483 (m), 1454 (m), 1414 (m), 1329 (m), 1288 (m), 1238 (w), 1153 (w), 1076 (s, br), 1009 (m), 930 (w), 903 (w), 845 (w), 814 (w), 740 (s), 656 (w), 621 (s), 579 (w), 565 (m), 527 (m), 509 (w), 488 (w), 447 (w), 415 (w), 322 (w), 285 (m). UV-Vis (20 °C, CH_3CN, nm) λ_{max} (ε, $M^{-1}cm^{-1}$): 248 (42400), 255 (43700), 267 (45300), 274 (53600), 281 (50500), 383 (410), 550 (211), 976 (16). CD (20 °C, CH_3CN, nm) λ (Δε, $M^{-1}cm^{-1}$): 258 (-47.7), 272 (-38.7), 279 (-30.0), 417 (-3.39), 515 (-0.58), 600 (-3.95). ESI-MS (soft positive mode, MeCN) m/z: 669.3 (86) $[Co^{III}(S\text{-}1\text{-}H)_2]^+$. Anal. Calculated for $[Co(S\text{-}1\text{-}H)_2][Co(S\text{-}1)_2](ClO_4)_3\cdot 0.5EtOH\cdot 1.5\ CH_2Cl_2$: C 49.25%, H 4.45%, N 12.68%; Found: C 49.21%, H 4.38%, N 12.25%.

Acknowledgements

This research was supported by the Swiss National Science Foundation.

Keywords: Transition metal complexes – Hydrogen bonding – chirality – magnetic exchange interactions – proton coupled electron transfer

References

[1] a) S. Yoshikawa and A. Shimada, *Chemical Reviews* **2015**, *115*, 1936-1989; b) S. Yoshikawa, K. Shinzawa-Itoh, E. Yamashita and T. Tsukihara, **2001**, pp. 348-362; c) M. Brunori, A. Giuffre and P. Sarti, *J. Inorg. Biochem.* **2005**, *99*, 324-336.

[2] a) B. Krebs and N. Straeter, *Angew. Chem.* **1994**, *106*, 889-891 (See also Angew. Chem., Int. Ed. Engl., 1994, 1933(1998), 1841-1993); b) J. D. Lipscomb and L. Que, Jr., *JBIC, J. Biol. Inorg. Chem.* **1998**, *3*, 331-336; c) D. A. Whittington, A. M. Valentine and S. J. Lippard, *JBIC, J. Biol. Inorg. Chem.* **1998**, *3*, 307-313; d) S. J. Lee, M. S. McCormick, S. J. Lippard and U.-S. Cho, *Nature* **2013**, *494*, 380-384.

[3] a) E. Gouré, B. Gerey, M. Clémancey, J. Pécaut, F. Molton, J.-M. Latour, G. Blondin and M.-N. Collomb, *Inorganic Chemistry* **2016**; b) S. M. Jansze, G. Cecot, M. D. Wise, K. O. Zhurov, T. K. Ronson, A. M. Castilla, A. Finelli, P. Pattison, E. Solari, R. Scopelliti, G. E. Zelinskii, A. V. Vologzhanina, Y. Z. Voloshin, J. R. Nitschke and K. Severin, *Journal of the American Chemical Society* **2016**, *138*, 2046-2054; c) M. Kuss-Petermann and O. S. Wenger, *Journal of the American Chemical Society* **2016**, *138*, 1349-1358; d) G. Passard, A. M. Ullman, C. N. Brodsky and D. G. Nocera, *Journal of the American Chemical Society* **2016**, *138*, 2925-2928; e) M. Schulze, V. Kunz, P. D. Frischmann and F. Würthner, *Nat Chem* **2016**, *8*, 576-583; f) B. Wurster, D. Grumelli, D. Hötger, R. Gutzler and K. Kern, *Journal of the American Chemical Society* **2016**, *138*, 3623-3626.

[4] a) C. Deville, M. Granelli, A. M. Downward, C. Besnard, L. Guenée and A. F. Williams, *Dalton Trans.* **2014**, *43*, 12917-12925; b) C. Deville, A. Spyratou, P. Aguirre-Etcheverry, C. Besnard and A. F. Williams, *Inorg. Chem.* **2012**, *51*, 8667-8669.

[5] G. A. van Albada, J. Reedijk, R. Hämäläinen, U. Turpeinen and A. L. Spek, *Inorg. Chim. Acta* **1989**, *163*, 213-222.

[6] K. Isele, V. Broughton, C. J. Matthews, A. F. Williams, G. Bernardinelli, P. Franz and S. Decurtins, *J. Chem. Soc. Dalton Trans.* **2002**, 3899-3905.

[7] K. Isele, F. Gigon, A. F. Williams, G. Bernardinelli, P. Franz and S. Decurtins, *Dalton Trans.* **2007**, 332-341.

[8] A. M. Downward, M. Granelli, C. Deville, L. Guenée, C. Besnard, A. Rodriguez Franco and A. F. Williams, *to be published*.

[9] P. L. Brown, R. N. Sylva and J. Ellis, *Journal of the Chemical Society, Dalton Transactions* **1985**, 723-730.

[10] a) G. Gilli and P. Gilli, *The Nature of the Hydrogen Bond, Outline of a comprehensive hydrogen bond theory*, Oxford University Press, **2009**, p; b) T. Steiner, *Angew. Chem. Int. Ed.* **2002**, *41*, 48-76; c) P. Gilli, L. Pretto, V. Bertolasi and G. Gilli, *Acc. Chem. Res.* **2009**, *42*, 33-44.

[11] S. G. Telfer and R. Kuroda, *Chemistry – A European Journal* **2005**, *11*, 57-68.

[12] a) M. Ardon and A. Bino, *Inorganic Chemistry* **1985**, *24*, 1343-1347; b) M. Ardon, A. Bino, K. Michelsen and E. Pedersen, *Journal of the American Chemical Society* **1987**, *109*, 5855-5856; c) U. Bossek, K. Wieghardt, B Nuber and J. Weiss, *Angewandte Chemie International Edition in English* **1990**, *29*, 1055-1057; d) P. A. Goodson, J. Glerup, D. J. Hodgson, K. Michelsen and U. Rychlewska, *Inorg. Chem.* **1994**, *33*, 359-366; e) M. Ardon, A. Bino, K. Michelsen, E. Pedersen and R. C. Thompson, *Inorg. Chem.* **1997**, *36*, 4147-4150; f) T. J. Morsing, H. Weihe and J. Bendix, *Inorganic Chemistry* **2016**, *55*, 1453-1460.

[13] a) W. Plass, A. Pohlmann and J. Rautengarten, *Angewandte Chemie International Edition* **2001**, *40*, 4207-4210; b) A. Okazawa and T. Ishida *Chem. Phys. Lett.* **2009**, *480*, 198-202; c) K. R. O'Neal, T. V. Brinzari, J. B. Wright, C. Ma, S. Giri, J. A. Schlueter, Q. Wang, P. Jena, Z. Liu and J. L. Musfeldt, *Scientific Reports* **2014**, *4*, 6054.

[14] a) S. Hill, R. S. Edwards, N. Aliaga-Alcalde and G. Christou, *Science* **2003** *302*, 1015-1018; b) W. Wernsdorfer, N. Aliaga-Alcalde, D. N. Hendrickson and G. Christou, *Nature* **2002**, *416*, 406-409.

[15] a) G. De Munno, W. Ventura, G. Viau, F. Lloret, J. Faus and M. Julve, *Inorganic Chemistry* **1998**, *37*, 1458-1464; b) Y. Ma, A.-L. Cheng and E.-Q. Gao, *Dalton Trans.* **2010**, *39*, 3521-3526; c) K. Wang, Y.-Q. Wang, X.-M. Zhang and E.-Q. Gao, *Dalton Trans.* **2013**, *42*, 4533-4538; d) I. Nemec, R. Herchel, T. Silha and Z. Travnicek, *Dalton Trans.* **2014**, *43*, 15602-15616.

[16] a) C. Desplanches, E. Ruiz, A. Rodriguez-Fortea and S. Alvarez, *J. Am. Chem. Soc.* **2002**, *124*, 5197-5205; b) N. A. G. Bandeira and B. L. Guennic, *J. Phys. Chem. A* **2012**, *116*, 3465-3473.

[17] C. Desplanches, E. Ruiz and S. Alvarez, *Chemical Communications* **2002**, 2614-2615.

[18] in *MAGMUM4.1/OW01*, *Vol.* pp. MAGMUN4.1/OW01.exe is available as a combined package free of charge from the authors (http://www.ucs.mun.ca/~lthomp/magmun). MAGMUM04.01 was developed by Dr. Z. Xu (Memorial University) and OW01.exe by Prof. O. Waldmann. Source codes are not distributed. The origin of the programme should be quoted. Spin state and energy calculations appropriate to a particular exchange Hamiltonian are calculated within the software, including the appropriate non-linear regressions using experimental variable temperature magnetic data. .

[19] a) S. Decurtins, H. U. Guedel and A. Pfeuti, *Inorganic Chemistry* **1982**, *21*, 1101-1106; b) S. Decurtins and H. U. Guedel, *Inorganic Chemistry* **1982**, *21*, 3598-3606.

[20] a) M. H. V. Huynh and T. J. Meyer, *Chem. Rev.* **2007**, *107*, 5004-5064; b) S. Hammes-Schiffer, *Chemical Reviews* **2010**, *110*, 6937-6938.

[21] a) I. Siewert, *Chem. - Eur. J.* **2015**, *21*, 15078-15091; b) S. J. Slattery, J. K. Blaho, J. Lehnes and K. A. Goldsby, *Coordination Chemistry Reviews* **1998**, *174*, 391-416.
[22] J. Rosenthal and D. G. Nocera, *Accounts of Chemical Research* **2007**, *40*, 543-553.
[23] J. L. Dempsey, J. R. Winkler and H. B. Gray, *Chemical Reviews* **2010**, *110*, 7024-7039.
[24] O. S. Wenger, *Chemistry – A European Journal* **2011**, *17*, 11692-11702.
[25] a) S. Hammes-Schiffer and A. A. Stuchebrukhov, *Chemical Reviews* **2010**, *110*, 6939-6960; b) S. Hammes-Schiffer, *Journal of the American Chemical Society* **2015**, *137*, 8860-8871.
[26] J. Bonin, C. Costentin, M. Robert, J.-M. Savéant and C. Tard, *Accounts of Chemical Research* **2012**, *45*, 372.
[27] J. Ruiz and D. Astruc, *C.R. Acad. Sci. Paris, Series II c* **1998**, *1*, 21-27.

10.1002/chem.201700591

WILEY-VCH

Entry for the Table of Contents)

FULL PAPER

A route to a series of dinuclear complexes held together by unusually strong hydrogen bonds is presented. The complexes show ferromagnetic or antiferromagnetic coupling through the bridge, and outer sphere electron transfer is facilitated by inner sphere proton transfer.

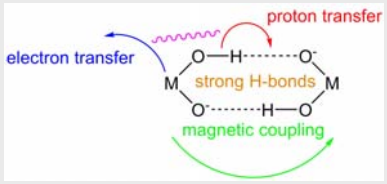

*Matteo Granelli, Alan M. Downward, Robin Huber, Laure Guénée, Céline Besnard, Karl W. Krämer, Silvio Decurtins, Shi-Xia Liu, Laurence K. Thompson and Alan F. Williams**

Page No. – Page No.

Dinuclear complexes formed by hydrogen bonds: synthesis, structure and magnetic and electrochemical properties.